

This is a repository copy of *Cluster expansion and vertex substitution pathways in nickel germanide Zintl clusters*.

White Rose Research Online URL for this paper:

<https://eprints.whiterose.ac.uk/175526/>

Version: Accepted Version

Article:

Townrow, Oliver P.E., Weller, Andrew orcid.org/0000-0003-1646-8081 and Goicoechea, Jose M. (2021) Cluster expansion and vertex substitution pathways in nickel germanide Zintl clusters. *Chemical communications*. ISSN 1364-548X

<https://doi.org/10.1039/D1CC02912F>

Reuse

Items deposited in White Rose Research Online are protected by copyright, with all rights reserved unless indicated otherwise. They may be downloaded and/or printed for private study, or other acts as permitted by national copyright laws. The publisher or other rights holders may allow further reproduction and re-use of the full text version. This is indicated by the licence information on the White Rose Research Online record for the item.

Takedown

If you consider content in White Rose Research Online to be in breach of UK law, please notify us by emailing eprints@whiterose.ac.uk including the URL of the record and the reason for the withdrawal request.

Cluster expansion and vertex substitution pathways in nickel germanide Zintl clusters

Oliver P. E. Townrow,^a Andrew S. Weller ^{*b} and Jose M. Goicoechea ^{*a}

Received 00th January 20xx,
Accepted 00th January 20xx

DOI: 10.1039/x0xx00000x

We describe the reactivity of the hypersilyl-functionalized Zintl cluster salt $K[Ge_9(Hyp)_3]$ towards the nickel reagents $Ni(COD)_2$ and $Ni(Cp)_2$, which gives rise to markedly different complexes. In the case of $Ni(COD)_2$ (COD = 1,5-cyclooctadiene), a dianionic sandwich-like cluster $[Ni\{Ge_9(Hyp)_3\}_2]^{2-}$ (**1**) was obtained, in line with a simple ligand substitution reaction of COD by $[Ge_9(Hyp)_3]^-$. By contrast, when an analogous reaction with $Ni(Cp)_2$ (Cp = cyclopentadienyl) was performed, vertex substitution of the $[Ge_9(Hyp)_3]^-$ precursor was observed, giving rise to the nine-vertex *nido*-cluster $(Cp)Ni[Ge_9(Hyp)_3]$ (**2**). This is the first instance of vertex substitution at a hypersilyl-functionalized Zintl cluster cage. The electrochemical behavior of these compounds was explored and showed reversible redox behaviour for both clusters.

Intermetallic materials consisting of nickel and germanium (nickel germanides) have been recently explored as catalysts,¹ components in microelectronics,² and thermoelectric materials.³ Methods for the preparation of such compounds include atomic layer deposition and direct current (DC) or radio frequency (RF) sputtering, which allow for the preparation of high purity samples. Given the important technological applications of such materials, the development of alternative synthetic techniques based on well-defined molecular precursors is an attractive prospect. In this context, one such family of compounds that are of interest are heteroatomic Zintl clusters composed of main group and transition metal elements.⁴ These soluble molecular species can be viewed as mimics of binary intermetallic compounds.⁵ As far as nickel germanide clusters are concerned, an array of species with varying compositions have been isolated to date such as $[Ni@Ge_9]^{3-}$,⁶ $[Ni@Ge_9Ni(CO)]^{3-}$,⁶ $[Ni_3@(Ge_9)_2]^{4-}$,⁷ and $[Ge_5Ni_2(CO)_3]^{2-}$.⁸ The formation of many of such clusters, $[Ni_2@Ge_{14}Ni_4(CO)_5]^{4-}$ for example,⁹ involves cluster-fragmentation pathways that are poorly understood owing to the lack of suitable spectroscopic handles to monitor such reactions. This aspect of Zintl cluster chemistry – the mechanisms by which an otherwise robust molecular precursor, such as the nonagermanide tetra-anion, $[Ge_9]^{4-}$, redistributes in solution to afford higher nuclearity clusters – remains for the most part a mystery, although recently some studies have aimed to elucidate viable pathways.¹⁰

In an effort to probe such reactivity, we have recently become interested in studying the tris-functionalised nonagermanide cluster $[Ge_9(Hyp)_3]^-$ (Hyp = Si(SiMe₃)₃).¹¹ Over the last ten years this species has received significant attention

as a supporting ligand for transition metals.^{12–15} For example, we recently reported its use in the synthesis of a novel Rh-based homogeneous catalyst for the hydrogenation of cyclic alkenes.¹⁵ The principal advantages of $[Ge_9(Hyp)_3]^-$ as a ligand are that it is (highly) soluble in non-polar aprotic solvents, and that reactions can be studied in greater detail using NMR techniques given the presence of ¹H and ²⁹Si nuclei in the hypersilyl substituents. A number of metal-containing clusters have been isolated containing this cluster as a support, that exhibit a variety of coordination modes (η^1 , η^3 , η^4 , η^5), which depend on the electronic requirement of the metal centres in question.^{12–15} Empirical observations also suggest that the $[Ge_9(Hyp)_3]^-$ precursor is less prone to fragmentation than that of its unsubstituted counterpart $[Ge_9]^{4-}$.^{4,16}

In addition to *cluster expansion* reactions, whereby higher nuclearity clusters form on reaction of Zintl clusters with transition metal reagents, another interesting class of reactions are those in which a transition metal fragment replaces one of the cluster vertices, so-called *vertex substitution* reactions.¹⁷ It has been postulated that vertex substitution of $[E_9]^{4-}$ clusters (E = Ge, Sn, Pb) may be an early step towards cluster expansion, whereby the fragmented cluster recombines with another to form higher nuclearity cages.^{10,18} Some examples of clusters which have undergone vertex substitution reactions include $[(Cp)Ti(Sn_8)]^{3-}$ and $[(CO)_3Fe(Ge_8)]^{3-}$,^{18,19} both of which exhibit cluster topologies encountered in higher nuclearity clusters such as $[Ni_2@Sn_{17}]^{4-}$.²⁰ The mechanisms involved in these processes remain poorly understood, largely because of the lack of methods to study the solution behaviour. Establishing complimentary reactivity in their functionalized, more soluble counterparts may allow us to monitor these processes.

Herein, we report the reactions of homoleptic nickel organometallics $Ni(COD)_2$ (COD = 1,5-cyclooctadiene) and $Ni(Cp)_2$ (Cp = cyclopentadienyl), both well studied precursors and dopants for Ni containing materials,^{21,22} with $K[Ge_9(Hyp)_3]$. These studies show that the nature of the nickel precursor has

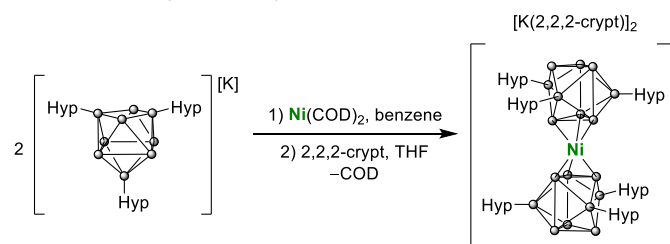
^a Department of Chemistry, University of Oxford, Chemistry Research Laboratory, 12 Mansfield Road, Oxford, OX1 3TA, U.K.

^b Department of Chemistry, University of York, YO10 5DD, U.K.

Electronic Supplementary Information (ESI) available: Experimental details, analytical data, spectra and computational methods. See DOI: 10.1039/x0xx00000x

a profound effect on the clusters formed in solution. Using $\text{Ni}(\text{COD})_2$ results in cluster expansion, while in contrast $\text{Ni}(\text{Cp})_2$ replaces one of the germanium vertices of the $[\text{Ge}_9(\text{Hyp})_3]^-$ cluster, in a vertex substitution reaction.

The reaction of $\text{Ni}(\text{COD})_2$ and two equivalents of $\text{K}[\text{Ge}_9(\text{Hyp})_3]$ in benzene or toluene results in the formation of a dark green solution, presumably of the complex $\text{K}_2[\text{Ni}\{\text{Ge}_9(\text{Hyp})_3\}_2]$ ($\text{K}_2[\mathbf{1}]$).[†] This product is unstable in solution for more than 2 days and also if placed under vacuum, forming a brown suspension from which the previously reported $[\text{K}(\text{tol})_3][\text{Ge}_9(\text{Hyp})_3] \cdot \text{tol}$ was recovered.²³ However, addition of 2,2,2-crypt (4,7,13,16,21,24-hexaoxa-1,10-diazabicyclo[8.8.8]-hexacosane) to the reaction mixture allows for the isolation of the dianionic formally Ni(0) sandwich compound $[\text{K}(2,2,2\text{-crypt})]_2[\text{Ni}\{\text{Ge}_9(\text{Hyp})_3\}_2]$ ($[\text{K}(2,2,2\text{-crypt})]_2[\mathbf{1}]$), which is sparingly soluble in THF (Scheme 1).



Scheme 1. Preparation of $[\text{K}(2,2,2\text{-crypt})]_2[\text{Ni}\{\text{Ge}_9(\text{Hyp})_3\}_2]$ ($[\text{K}(2,2,2\text{-crypt})]_2[\mathbf{1}]$).

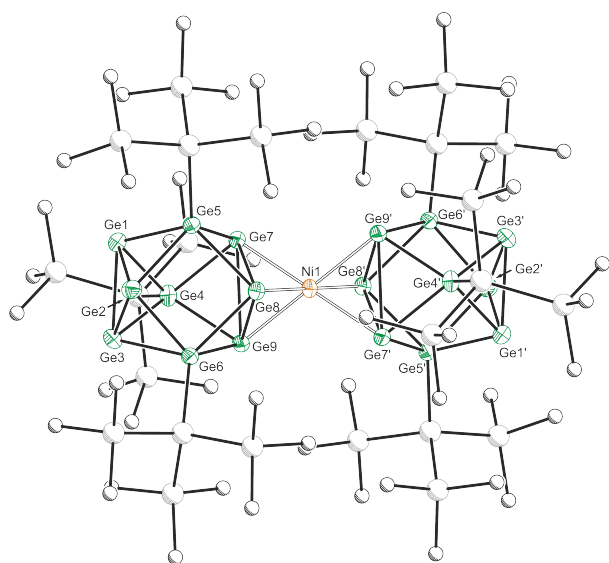


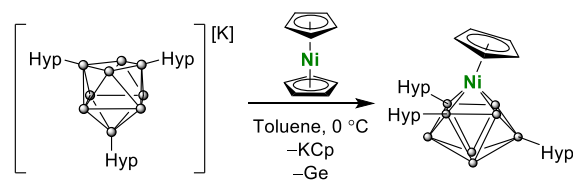
Figure 1. Molecular structure of $[\text{K}(2,2,2\text{-crypt})]_2[\mathbf{1}] \cdot 2\text{THF}$. Anisotropic displacement ellipsoids are set at 50% probability. Hydrogen atoms, $[\text{K}(2,2,2\text{-crypt})]^+$, and solvent of crystallisation have been omitted for clarity. Carbon and silicon atoms are pictured as spheres of arbitrary radii. Selected bond distances [Å]: Ni1–Ge7: 2.442(1), Ni1–Ge8: 2.436(1), Ni1–Ge9: 2.443(1), Ge1–Ge2: 2.679(1), Ge1–Ge3: 2.643(1), Ge2–Ge3: 2.631(1), Ge7–Ge8: 2.900(1), Ge7–Ge9: 2.830(1), Ge8–Ge9: 2.826(1). Symmetry operation $\bar{1}$: $1-x, 1-y, -z$.

Dark green-blue crystals suitable for single crystal X-ray crystallography were grown from a concentrated THF solution at -40°C . The cluster adopts a D_{3d} symmetric sandwich-like geometry in which the central Ni atom is coordinated by a triangular face of each of the two flanking clusters (Figure 1). The coordinated Ge–Ge distances are elongated by ~ 0.2 Å compared with the non-coordinated face of the cluster. The

dianionic cluster $\mathbf{1}$ is valence isoelectronic with related clusters such $[\text{M}[\text{Ge}_9(\text{Hyp})_3]_2]$ ($\text{M} = \text{Zn-Hg}$) and $[\text{Au}[\text{Ge}_9(\text{Hyp})_3]_2]^{-13i,j}$. There is also a close structural relationship to the substituent-free species $[\text{Ni}_3@(\text{Ge}_9)_2]^{4-,7}$ although it is notable that the Ni–Ge bond lengths in $\mathbf{1}$ are ca. 0.1 Å shorter, 2.436(1)–2.443(1) Å, (cf. 2.505(1)–2.540(1) Å in $[\text{Ni}_3@(\text{Ge}_9)_2]^{4-}$), which is presumably due to the absence of interstitial nickel atoms in the former, and its reduced overall charge.

NMR spectroscopic analysis of $\mathbf{1}$ shows one hypersilyl singlet resonance in the ^1H NMR spectrum at 0.38 ppm as well as resonances at 2.58, 3.57 and 3.61 ppm from the two $[\text{K}(2,2,2\text{-crypt})]^+$ counter-ions. $^{13}\text{C}\{^1\text{H}\}$ and $^1\text{H}/^{29}\text{Si}$ HMBC NMR spectra are in agreement with retention of the D_{3d} geometry in solution, the latter exhibiting two ^{29}Si NMR resonances with two cross-peaks. This is as expected from the symmetry observed in the solid state. Owing to decomposition via fragmentation in solution, a small amount ($\sim 3\%$) of the previously reported $[\text{K}(2,2,2\text{-crypt})][\text{Ge}_9(\text{Hyp})_3]$ is also present (see ESI).

In an attempt to isolate a mixed sandwich complex, we turned our attention to the reaction of $\text{Ni}(\text{Cp})_2$ and $(\text{Cp})\text{Ni}(\text{PPh}_3)\text{Cl}$ with $\text{K}[\text{Ge}_9(\text{Hyp})_3]$, however both reactions resulted in vertex substitution, whereby a germanium atom of the cluster cage is replaced by a $(\text{Cp})\text{Ni}$ fragment, producing the neutral cluster $(\text{Cp})\text{Ni}[\text{Ge}_8(\text{Hyp})_3]$ ($\mathbf{2}$). Vertex substitution has been previously observed for unsubstituted $[\text{E}_9]^{4-}$ ($\text{E} = \text{Ge}, \text{Sn}$) clusters,^{17–19} performed in highly polar solvents under reducing conditions, however such transformations are unprecedented for functionalized precursors such as $[\text{Ge}_9(\text{Hyp})_3]^-$.



Scheme 2. Preparation of $(\text{Cp})\text{Ni}[\text{Ge}_8(\text{Hyp})_3]$ ($\mathbf{2}$).

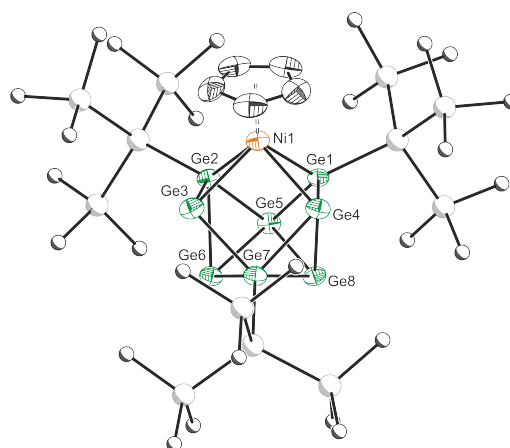


Figure 2. Molecular structure of $\mathbf{2} \cdot 1.5\text{tol}$. Anisotropic displacement ellipsoids are set at 50% probability. Hydrogen atoms and solvent of crystallisation have been omitted for clarity. Carbon and silicon atoms are pictured as spheres of arbitrary radii. Selected bond distances [Å]: Ni1–Ge1: 2.400(2); Ni1–Ge2: 2.404(2); Ni1–Ge3: 2.591(2); Ni1–Ge4: 2.580(2).

Emerald green crystals of $\mathbf{2}$ suitable for single crystal X-ray crystallography were grown from a concentrated solution of

toluene. The cluster adopts a C_5 -symmetric distorted mono-capped square-antiprismatic geometry. This cluster can be described as a *nido*-deltahedron with 22 electrons available for cluster bonding.²⁴ Structurally, this cluster is closely related to $[(\text{Cp})\text{Ti}(\text{Sn}_8)]^{3-}$ and $[(\text{CO})_3\text{Fe}(\text{Ge}_8)]^{3-}$.^{18,19}

NMR spectroscopy is in agreement with the solid state structure, exhibiting two ^1H NMR resonances for the hypersilyl environments at 0.49 and 0.60 ppm in a 2:1 ratio, in addition to a single resonance for the C_5H_5 ligand at 5.18 ppm. In addition to this, $^{13}\text{C}\{^1\text{H}\}$ and $^1\text{H}/^{29}\text{Si}$ HMBC NMR supply further evidence for the two inequivalent hypersilyl environments, with four cross peaks observed in the HMBC spectrum.

The structural relationship and contrasting electron counts between **2** and $[(\text{CO})_3\text{Fe}(\text{Ge}_8)]^{3-}$ (22 and 21 cluster bonding electrons, respectively), point to the possibility of facile redox processes. We were intrigued to explore the electrochemical behaviour of these clusters through a series of cyclic voltammetry (CV) studies.

The dianionic sandwich complex **1** features a reversible oxidation at $E_1^0 = -1.56$ V (Figure 3), which is followed by a second, quasi-reversible oxidation event at $E_2^0 = -1.20$ V (all potentials given relative to the ferrocene/ferrocenium redox couple; $\text{Fc}^{0/+} = 0$). This is followed by a third oxidation ($E_3^{\text{pa}} = -0.85$ V vs. $\text{Fc}^{0/+}$) which is irreversible at all scan rates ($v = 0.05$ – 1 mVs $^{-1}$). To date, this is only the second observation of reversible redox behaviour for solutions of Zintl clusters.²⁵ However, attempts to chemically access these oxidized clusters by, for example, oxidation with cobaltocenium hexafluorophosphate were unsuccessful. This leads us to believe that while oxidized clusters may be kinetically accessible, they cannot be accessed because of decomposition.

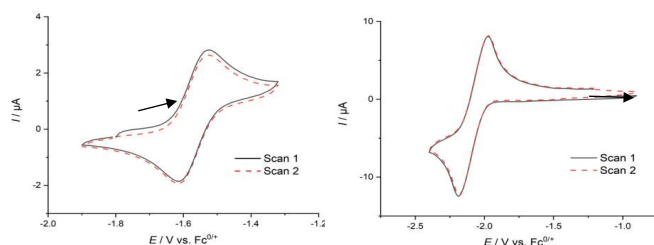


Figure 3. Cyclic voltammogram of complexes **1** (left; 100 mV/s; first oxidative event; 1.0 mM, 0.2 M $[\text{NBu}_4][\text{PF}_6]$, THF, room temperature) and **2** (right; 100 mV/s; first reductive event; 1.0 mM, 0.1 M $[\text{NBu}_4][\text{PF}_6]$, THF, room temperature).

Electrochemical analysis of **2** features a reversible reductive event at $E_1^0 = -2.07$ V. This is followed by a second reduction at $E_2^{\text{pc}} = -2.54$ V, which is irreversible at all scan rates ($v = 0.05$ – 1 mVs $^{-1}$) and is accompanied by two additional irreversible features in the reverse scan ($E^{\text{pa}} = -2.38$, -1.21 V) indicating some form of cluster degradation/rearrangement on over-reduction. Attempts to access this compound via reduction with a Na/Hg amalgam gave rise to a complex ^1H NMR spectrum, indicative of excessive cluster decomposition. As with **1**, it would appear that while these reversible reductive redox events are observable in the cyclic voltammetry measurements, chemical isolation of these compounds is challenging. Interestingly, and despite the precedent for a closely related

oxidized cluster, $[(\text{CO})_3\text{Fe}(\text{Ge}_8)]^{3-}$, no oxidation events were observed in the CV scans.

Conclusions

We have shown that two distinct reactivity pathways are accessible for the functionalised Zintl cluster $[\text{Ge}_9(\text{Hyp})_3]^-$ on reaction with nickel reagents. In the case of the nickel(0) precursor $\text{Ni}(\text{COD})_2$ simple ligand displacement gives rise to the sandwich type compound $[\text{Ni}\{\text{Ge}_9(\text{Hyp})_3\}_2]^{2-}$, and cluster expansion. By contrast, reactions with the nickel(II) reagents $\text{Ni}(\text{Cp})_2$ and $(\text{Cp})\text{Ni}(\text{PPh}_3)\text{Cl}$ were found to give rise to vertex-substitution reactions, whereby a germanium atom of the $[\text{Ge}_9(\text{Hyp})_3]^-$ cluster is replaced by a $\text{Ni}(\text{Cp})$ moiety. This is the first example of such a transformation involving functionalized Zintl clusters such as $[\text{Ge}_9(\text{Hyp})_3]^-$. While the reaction mechanism for such a transformation remains unknown, the high yield in which this compound can be obtained should allow for further reactivity studies.

Conflicts of interest

There are no conflicts to declare.

Acknowledgements

We thank Shell Global Solutions International B.V., the EPSRC and the University of Oxford for financial support of this research (Industrial CASE studentship O.P.E.T.). The University of Oxford is also acknowledged for access to Chemical Crystallography facilities.

Notes and references

‡ See ESI for all experimental details.

- (a) J. Y. Chen, S. Lou Jheng and H. Y. Tuan, *Nanoscale*, 2018, **10**, 11072–11078; (b) P. W. Menezes, S. Yao, R. Beltrán-Suito, J. N. Hausmann, P. V. Menezes and M. Driess, *Angew. Chem. Int. Ed.*, 2021, **60**, 4640–4647.
- (a) B. De Schutter, K. Van Stiphout, N. M. Santos, E. Bladt, J. Jordan-Sweet, S. Bals, C. Lavoie, C. M. Comrie, A. Vantomme, and C. Detavernier, *J. Appl. Phys.*, 2016, **119**, 135305; (b) T. Grzela, G. Capellini, W. Koczorowski, M. A. Schubert, R. Czajka, N. J. Curson, I. Heidmann, T. Schmidt, J. Falta and T. Schroeder, *Nanotechnology*, 2015, **26**, 385701; (c) M. Sheehan, Y. Guo, G. Flynn, H. Geaney and K. M. Ryan, *CrystEngComm*, 2017, **19**, 2072–2078; (d) M. Swain, S. Singh, D. Bhattacharya, A. Singh, R. B. Tokas, C. L. Prajapat and S. Basu, *AIP Adv.*, 2015, **5**, 077129; (e) C. Yan, J. M. Higgins, M. S. Faber, P. S. Lee and S. Jin, *ACS Nano*, 2011, **5**, 5006–5014; (f) S. Zhu and A. Nakajima, *Japanese J. Appl. Physics, Part 2 Lett.*, 2005, **44**, L753.
- (a) K. Kim, S. Mun, M. Jang, J. Sok and K. Park, *Appl. Phys. A Mater. Sci. Process.*, 2021, **127**, 50; (b) M. Noroozi, B. Hamawandi, M. S. Toprak and H. H. Radamson, in *ULIS 2014 - 2014 15th Int. Conf. Ultim. Integr. Silicon*, IEEE Computer Society, 2014, pp. 125–128.
- For review articles see: (a) B. Weinert, S. Mitzinger and S. Dehnen, *Chem. Eur. J.*, 2018, **24**, 8470–8490; (b) R. J. Wilson,

- B. Weinert and S. Dehnen, *Dalton Trans.*, 2018, **47**, 14861–14869. (c) B. Weinert and S. Dehnen, *Struct. Bond*, 2017, **174**, 99–134; (d) N. Korber, *Angew. Chem. Int. Ed.*, 2009, **48**, 3216–3217; (e) S. C. Sevov and J. M. Goicoechea, *Organometallics*, 2006, **25**, 5678–5692.
- 5 For a recent review of intermetalloid clusters see: K. Mayer, J. Weßing, T. F. Fässler and R. A. Fischer, *Angew. Chem. Int. Ed.* 2018, **57**, 14372–14393.
 - 6 J. M. Goicoechea and S. C. Sevov, *J. Am. Chem. Soc.*, 2006, **128**, 4155–4161.
 - 7 J. M. Goicoechea and S. C. Sevov, *Angew. Chem. Int. Ed.*, 2005, **117**, 4094–4096.
 - 8 C. Liu, L. J. Li, Q. J. Pan and Z. M. Sun, *Chem. Commun.*, 2017, **53**, 6315–6318.
 - 9 E. N. Esenturk, J. Fettinger and B. Eichhorn, *Polyhedron*, 2006, **25**, 521–529.
 - 10 (a) C. Zhang, H. W. T. Morgan, Z. C. Wang, C. Liu, Z. M. Sun and J. E. McGrady, *Dalton Trans.*, 2019, **48**, 15888–15895; (b) S. Mitzinger, L. Broeckert, W. Massa, F. Weigend and S. Dehnen, *Nat. Commun.*, 2016, **7**, 1–10; (c) J. Q. Wang, S. Stegmaier, B. Wahl and T. F. Fässler, *Chem. Eur. J.*, 2010, **16**, 1793–1798.
 - 11 (a) F. Li and S. C. Sevov, *Inorg. Chem.*, 2012, **51**, 2706–2708; (b) A. Schnepf, *Angew. Chem. Int. Ed.*, 2003, **42**, 2624–2625.
 - 12 For examples of η^1 -[Ge₉R₃]⁻ clusters see: (a) F. S. Geitner, W. Klein, O. Storcheva, T. D. Tilley and T. F. Fässler, *Inorg. Chem.*, 2019, **58**, 13293–13298; (b) N. C. Michenfelder, C. Gienger, A. Schnepf and A. N. Unterreiner, *Dalton Trans.*, 2019, **48**, 15577–15582;
 - 13 For examples of η^3 -[Ge₉R₃]⁻ clusters see: (a) L. J. Schiegerl, M. Melaimi, D. R. Tolentino, W. Klein, G. Bertrand and T. F. Fässler, *Inorg. Chem.*, 2019, **58**, 3256–3264; (b) O. Kysliak, D. D. Nguyen, A. Z. Clayborne and A. Schnepf, *Inorg. Chem.*, 2018, **57**, 12603–12609; (c) F. S. Geitner, M. A. Giebel, A. Pöthig and T. F. Fässler, *Molecules*, 2017, **22**, 1204; (d) F. S. Geitner and T. F. Fässler, *Eur. J. Inorg. Chem.*, 2016, **2016**, 2688–2691; (e) O. Kysliak, C. Schrenk and A. Schnepf, *Chem. Eur. J.*, 2016, **22**, 18787–18793; (f) K. Mayer, L. J. Schiegerl and T. F. Fässler, *Chem. Eur. J.*, 2016, **22**, 18794–18800; (g) F. Li and S. C. Sevov, *Inorg. Chem.*, 2015, **54**, 8121–8125; (h) C. Schenk, F. Henke, G. Santiso-Quiñones, I. Krossing and A. Schnepf, *Dalton Trans.*, 2008, 4436–4441; (i) F. Henke, C. Schenk and A. Schnepf, *Dalton Trans.*, 2009, 9141–9145; (j) C. Schenk and A. Schnepf, *Angew. Chem. Int. Ed.*, 2007, **46**, 5314–5316.
 - 14 For examples of η^5 -[Ge₉R₃]⁻ clusters see: (a) S. Frischhut, F. Kaiser, W. Klein, M. Drees, F. E. Kühn and T. F. Fässler, *Organometallics*, 2018, **37**, 4560–4567; (b) F. Li, A. Muñoz-Castro and S. C. Sevov, *Angew. Chem. Int. Ed.*, 2016, **55**, 8630–8633; (c) F. Henke, C. Schenk and A. Schnepf, *Dalton Trans.*, 2011, **40**, 6704–6710; (d) C. Schenk and A. Schnepf, *Chem. Commun.*, 2009, 3208–3210;
 - 15 O. P. E. Townrow, C. Chung, S. A. Macgregor, A. S. Weller and J. M. Goicoechea, *J. Am. Chem. Soc.*, 2020, **142**, 18330–18335.
 - 16 D. R. Gardner, J. C. Fettinger and B. W. Eichhorn, *Angew. Chem. Int. Ed.*, 1996, **35**, 2852–2854.
 - 17 For a recent example of vertex substitution reactions in Zintl cluster chemistry see: A. M. Li, Y. Wang, P. Y. Zavalij, F. Chen, A. Muñoz-Castro and B. W. Eichhorn, *Chem. Commun.*, 2020, **56**, 10859–10862.
 - 18 C. B. Benda, M. Waibel and T. F. Fässler, *Angew. Chem. Int. Ed.*, 2015, **54**, 522–526.
 - 19 B. Zhou and J. M. Goicoechea, *Chem. Eur. J.*, 2010, **16**, 11145–11150.
 - 20 E. N. Esenturk, A. J. C. Fettinger and B. W. Eichhorn, *J. Am. Chem. Soc.*, 2006, **128**, 12–13.
 - 21 (a) J. Bachmann, A. Zolotaryov, O. Albrecht, S. Goetze, A. Berger, D. Hesse, D. Novikov and K. Nielsch, *Chem. Vap. Depos.*, 2011, **17**, 177–180; (b) S.-D. Hwang, *J. Vac. Sci. Technol. B Microelectron. Nanom. Struct.*, 1996, **14**, 2957; (c) M. V. Kharlamova, M. Sauer, T. Saito, Y. Sato, K. Suenaga, T. Pichler and H. Shiozawa, *Nanoscale*, 2015, **7**, 1383–1391; (d) J. A. Singh, N. F. W. Thissen, W. H. Kim, H. Johnson, W. M. M. Kessels, A. A. Bol, S. F. Bent and A. J. M. Mackus, *Chem. Mater.*, 2018, **30**, 663–670.
 - 22 (a) J. S. Bradley, B. Tesche, W. Busser, M. Maase and M. T. Reetz, *J. Am. Chem. Soc.*, 2000, **122**, 4631–4636; (b) N. J. S. Costa, R. F. Jardim, S. H. Masunaga, D. Zanchet, R. Landers and L. M. Rossi, *ACS Catal.*, 2012, **2**, 925–929; (c) T. O. Ely, C. Amiens, B. Chaudret, E. Snoeck, M. Verelst, M. Respaud and J. M. Broto, *Chem. Mater.*, 1999, **11**, 526–529.
 - 23 O. Kysliak and A. Schnepf, *Dalton Trans.*, 2016, **45**, 2404–2408.
 - 24 T. A. Albright, J. K. Burdett and M. H. Whangbo, *Orbital Interactions in Chemistry: Second Edition*, 2013.
 - 25 J. M. Goicoechea and S. Sevov, *Inorg. Chem.*, 2005, **44**, 2654–2658.